



Deposited via The University of Leeds.

White Rose Research Online URL for this paper:

<https://eprints.whiterose.ac.uk/id/eprint/134589/>

Version: Accepted Version

Article:

Guedes, AF, Carvalho, FA, Domingues, MM et al. (2018) Sensing adhesion forces between erythrocytes and γ ' fibrinogen, modulating fibrin clot architecture and function. *Nanomedicine: Nanotechnology, Biology and Medicine*, 14 (3). pp. 909-918. ISSN: 1549-9634

<https://doi.org/10.1016/j.nano.2018.01.006>

© 2018 Elsevier Inc. Licensed under the Creative Commons Attribution-Non Commercial No Derivatives 4.0 International License (<https://creativecommons.org/licenses/by-nc-nd/4.0/>).

Reuse

This article is distributed under the terms of the Creative Commons Attribution-NonCommercial-NoDerivs (CC BY-NC-ND) licence. This licence only allows you to download this work and share it with others as long as you credit the authors, but you can't change the article in any way or use it commercially. More information and the full terms of the licence here: <https://creativecommons.org/licenses/>

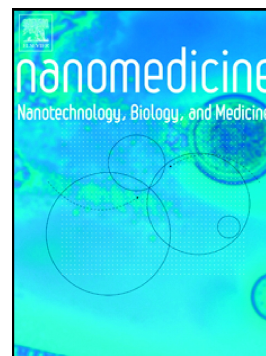
Takedown

If you consider content in White Rose Research Online to be in breach of UK law, please notify us by emailing eprints@whiterose.ac.uk including the URL of the record and the reason for the withdrawal request.

Accepted Manuscript

Sensing adhesion forces between erythrocytes and γ' fibrinogen, modulating fibrin clot architecture and function

Ana Filipa Guedes, Filomena A. Carvalho, Marco M. Domingues, Fraser L. Macrae, Helen R. McPherson, Nuno C. Santos, Robert A.S. Ariëns



PII: S1549-9634(18)30017-0
DOI: <https://doi.org/10.1016/j.nano.2018.01.006>
Reference: NANO 1740

To appear in:

Received date: 11 April 2017
Revised date: 12 December 2017
Accepted date: 11 January 2018

Please cite this article as: Ana Filipa Guedes, Filomena A. Carvalho, Marco M. Domingues, Fraser L. Macrae, Helen R. McPherson, Nuno C. Santos, Robert A.S. Ariëns, Sensing adhesion forces between erythrocytes and γ' fibrinogen, modulating fibrin clot architecture and function. The address for the corresponding author was captured as affiliation for all authors. Please check if appropriate. Nano(2018), <https://doi.org/10.1016/j.nano.2018.01.006>

This is a PDF file of an unedited manuscript that has been accepted for publication. As a service to our customers we are providing this early version of the manuscript. The manuscript will undergo copyediting, typesetting, and review of the resulting proof before it is published in its final form. Please note that during the production process errors may be discovered which could affect the content, and all legal disclaimers that apply to the journal pertain.

Sensing adhesion forces between erythrocytes and γ' fibrinogen, modulating fibrin clot architecture and function

Ana Filipa Guedes^{1,2}, Filomena A. Carvalho¹, Marco M. Domingues^{1,2}, Fraser L. Macrae², Helen R. McPherson², Nuno C. Santos^{1,*#}, Robert A. S. Ariens^{2,*#}

* Equal contribution

¹Instituto de Medicina Molecular, Faculdade de Medicina, Universidade de Lisboa, Lisbon, Portugal; ²Thrombosis and Tissue Repair Group, Division of Cardiovascular and Diabetes Research, Leeds Institute of Cardiovascular and Metabolic Medicine and Multidisciplinary Cardiovascular Centre, Faculty of Medicine and Health, University of Leeds, Leeds, United Kingdom.

[#]To whom correspondence should be addressed:

Robert Ariens, Thrombosis and Tissue Repair Group, Division of Cardiovascular and Diabetes Research, Leeds Institute of Cardiovascular and Metabolic Medicine, Faculty of Medicine and Health, University of Leeds, Leeds, Clarendon Way, Leeds LS2 9JT, United Kingdom; Tel: (+44)1133437734, Fax: (+44) 1133437738; Email: r.a.s.ariens@leeds.ac.uk.

Nuno C. Santos, Instituto de Medicina Molecular, Faculdade de Medicina, Universidade de Lisboa, Av. Prof. Egas Moniz, 1649-028 Lisboa, Portugal; Tel.: (+351)217999480; Fax: (+351) 217999477; E-mail: nsantos@medicina.ulisboa.pt

Abstract word count: 132

Complete manuscript word count: 4949

Number of references: 48

Number of figures/tables: 7

Funding: This work was supported by Fundação para a Ciência e a Tecnologia – Ministério da Ciência, Tecnologia e Ensino Superior (FCT-MCTES, Portugal; PTDC/QUI-BIQ/119509/2010, PTDC/BBB-BMD/6307/2014 and SFRH/BD/84414/2012), the British Heart Foundation (RG/13/3/30104) and the Garfield Weston Trust.

Conflicts of interest: The authors have no conflicts of interest to disclose.

Abbreviations: γ' , gamma prime fibrinogen; AFM, atomic force microscopy; γ A, the most common fibrinogen variant; RBCs, red blood cells; CVD, cardiovascular diseases; FXIII, factor XIII; SEM, scanning electron microscopy, LSCM, laser scanning confocal microscopy.

Abstract

Plasma fibrinogen includes an alternatively spliced γ -chain variant (γ'), which mainly exists as a heterodimer ($\gamma A\gamma'$) and has been associated with thrombosis. We tested $\gamma A\gamma'$ fibrinogen-red blood cells (RBCs) interaction using atomic force microscopy-based force spectroscopy, magnetic tweezers, fibrin clot permeability, scanning electron microscopy and laser scanning confocal microscopy. Data reveal higher work necessary for RBC-RBC detachment in the presence of $\gamma A\gamma'$ rather than $\gamma A\gamma A$ fibrinogen. $\gamma A\gamma'$ fibrinogen-RBCs interaction is followed by changes in fibrin network structure, which forms an heterogeneous clot structure with areas of denser and highly branched fibrin fibers. The presence of RBCs also increased the stiffness of $\gamma A\gamma'$ fibrin clots which are less permeable and more resistant to lysis than $\gamma A\gamma A$ clots. The modifications on clots promoted by RBCs- $\gamma A\gamma'$ fibrinogen interaction could alter the risk of thrombotic disorders.

Keywords: cell adhesion, atomic force microscopy, magnetic tweezers, fibrin clot, γ' fibrinogen.

Background

Fibrinogen is a 340 kDa homodimeric plasma glycoprotein, composed of three pairs of polypeptide chains, denoted A α , B β and γ , linked together by 29 disulphide bonds¹. A common variant of the fibrinogen is produced by alternative splicing of mRNA of the γ -chain, called γ' fibrinogen². The γ' isoform has a substitution of the final 4 carboxyl-terminal amino acid residues (AGDV) of the prevalent γ A-chain with a different 20-amino acid residue sequence (VRPEHPAETEYDSLYPEDDL), which includes a high proportion of negatively charged residues and two sulfated tyrosines. This variant accounts for 8-15% of all plasma fibrinogen, largely in the form of the heterodimer γ A γ' , while the homodimer $\gamma'\gamma'$ accounts for less than 1% of total plasma fibrinogen³. γ' fibrinogen has distinct biochemical and biophysical properties that distinguish it from the more common γ A isoform^{4, 5, 6}. Studies have highlighted that abnormal plasma levels of γ A γ' fibrinogen are associated with thrombotic diseases, such as coronary artery disease⁷, myocardial infarction⁸ and stroke⁹. Elevated levels of γ' fibrinogen in patients with cardiovascular disease (CVD) were independent of the total plasma fibrinogen concentration⁷. This could indicate that the proportion of γ' variant in plasma may be a risk factor for cardiovascular pathologies. However, reduced concentrations have been associated with microangiopathy syndrome¹⁰ and deep vein thrombosis¹¹. Studies by Appiah *et al.* did not support the hypothesis that γ' fibrinogen influences CVD events through its prothrombotic properties. Rather, γ' fibrinogen concentrations seem to reflect general inflammation that accompanies and may contribute to atherosclerotic CVD, instead of γ' fibrinogen being a causal risk factor¹². In addition to this, Walton *et al.* found that elevated levels of γ A γ A fibrinogen promoted arterial thrombosis *in vivo*, whereas γ A γ' fibrinogen did not¹³. Nevertheless, as γ' chain modulates clot formation *in vitro*, further studies are required to elucidate its functional properties and its possible relationship with bleeding disorders or thrombosis.

The formation of a thrombus and subsequent impairment of blood flow to vital organs are the immediate cause of CVD events¹⁴. The architecture of the clot network affects clot stability, particularly its viscoelastic or mechanical properties and fibrinolytic characteristics^{15, 16}. These

aspects can determine if the clot is broken down by fibrinolysis or if it will lead to occlusion or embolization¹⁷. Other studies have indicated the clinical relevance of fibrin clot structure. It has been shown that tightly packed and rigid clots with thinner fibers and low porosity are less susceptible to the action of thrombolytic agents^{18, 19}, and a prolonged clot lysis time has been associated with CVD events²⁰. Several studies have shown that clots produced from $\gamma A\gamma'$ fibrinogen have a different structure and behave differently from $\gamma A\gamma A$ clots^{4, 5, 6}. Fibrin clots formed in the presence of the fibrinogen γ' variant are more resistant to fibrinolysis, due to reduced binding of plasminogen and tissue plasminogen activator, leading to reduced plasmin generation²¹. Fibrinogen γ' variant is associated with a heterogeneous, non-uniform clot structure, with more branch points than clots formed by γA chains^{6, 22, 23}. In addition, γ' fibrinogen binds to thrombin exosite II²⁴. The binding of thrombin to the γ' chain has been reported to modulate thrombin activity, particularly towards substrates that require exosite II interaction such as coagulation factors FV and FVIII (but not those dependent on exosite I interactions, e.g. fibrinogen and factor FXIII), which may influence clot structure⁶. However, some of the effects of γ' fibrinogen on clot structure have been shown to be independent of thrombin, as clots produced with snake venom enzyme ancrod, which cleaves fibrinopeptide A from fibrinogen but not fibrinopeptide B, show similar structural abnormalities as those produced with thrombin²². On the other hand, it has been shown that the high affinity binding of thrombin to $\gamma A\gamma'$ -fibrin protects thrombin from inhibition by antithrombin, raising the possibility that $\gamma A\gamma'$ -fibrin serves as a scavenger and reservoir for thrombin in the clot²⁵.

Fibrinogen is thought to contribute to CVD, not only through altering the fibrin network structure, but also through several other mechanisms, such as promoting red blood cell (RBC) aggregation²⁶. Although several studies on isolated fibrin clots have been performed, *in vitro* experiments using fibrin blood clots containing RBCs are scarce in the literature. RBCs play a role in blood coagulation by increasing blood viscosity, which is associated with propensity for clot formation²⁷. RBCs have been shown to interact specifically with fibrinogen, with *ca.*20,000 binding sites *per* RBC and a dissociation constant, K_d , of approximately $1.3 \mu M$ ²⁸. We have identified a specific receptor for fibrinogen on the surface of RBCs^{29, 30, 31}.

Despite their significance in thrombosis and hemostasis, relatively few studies have been conducted to describe the effects of RBCs on blood clot structure, particularly with different fibrinogen variants. One complication of studying RBC-rich thrombi is that incorporation of RBCs into a thrombus seems uncontrolled and variable. This scarcity may also be, in part, due to the fact that the presence of RBCs in a clot often interferes with the techniques available to monitor clot structure³².

The present study aimed to investigate, through atomic force microscopy-based force spectroscopy, the adhesion of RBCs in the presence of $\gamma A\gamma A$ or $\gamma A\gamma'$ fibrinogen variants. Moreover, we aimed to understand the effect of RBC- $\gamma A\gamma'$ fibrinogen interactions on fibrin clot structure, properties and function through scanning electron microscopy, laser scanning confocal microscopy, magnetic tweezers and permeability studies.

Methods

Purification of $\gamma A\gamma A$ and $\gamma A\gamma'$ fibrinogen

The $\gamma A\gamma A$ and $\gamma A\gamma'$ fibrinogen variants were purified from human plasminogen-depleted fibrinogen using anion-exchange chromatography (Millipore, Billerica, MA) as previously described^{22, 23}. Detailed description of the method can be found in Supplementary Material.

Human RBCs isolation

Blood from healthy donors was obtained, with written informed consent, at the Instituto Português do Sangue e da Transplantação (IPST, Lisbon) and at the University of Leeds. This study was approved by the joint Ethics Committee of Faculdade de Medicina da Universidade de Lisboa and Centro Hospitalar Lisboa Norte, and by the University of Leeds Medical School Ethical Committee. RBCs were isolated through standard procedures^{29, 30, 31}.

Atomic force microscopy (AFM) – Cell-Cell adhesion

AFM studies were performed on a NanoWizard II atomic force microscope with a CellHesion 200 module (JPK Instruments, Berlin, Germany), mounted on an Axiovert200 inverted optical microscope (Zeiss, Jena, Germany). RBCs were attached to tipless cantilevers through the functionalization with concanavalin A (for details see Supplementary Material). RBCs on the substrate were adhered to poly-L-lysine coated glass slides. RBC-RBC adhesion was measured in the presence of different fibrinogen variant concentrations, from 0 to 1.0 mg/ml. Detailed description of the method can be found in Supplementary Material.

Magnetic tweezers

To examine the viscoelastic properties of the fibrin clots, magnetic tweezers were used. The magnetic microrheometer operates by applying a force of 40 pN to a 4.5 μm superparamagnetic bead (Dynabeads M-450 Epoxy, Invitrogen, Paisley, UK) using a magnetic field gradient generated by four electromagnets in 2D directions. The device was used coupled with an

Olympus IX71 inverted microscope (Olympus, UK) incorporating an ultralong working objective (40× magnification) and a CCD camera. Particle tracking, electromagnet control and image analysis were performed in real time using custom written Labview 7.1 software (National Instruments, Newbury, UK). Fibrin clots were formed with and without RBCs. The viscoelastic properties were measured using the procedure of Evans *et al.*³³. The parameters G' , G'' and $\tan \delta$ were calculated at a frequency of 0.1 Hz. The displacement of 8 random magnetic beads was measured *per* sample, and each sample was studied at least in triplicate. Please find detailed description in Supplementary Material.

Fibrin clot permeability

To study the clot permeability, samples were prepared in triplicate, according to the standardized protocol published by the Fibrinogen and FXIII Subcommittee of the International Society on Thrombosis and Hemostasis (ISTH)³⁴. Purified fibrinogen samples (final concentration of 1 mg/ml) were incubated with 1 U/ml human thrombin (Calbiochem, Nottingham, UK) and 2.5 mM CaCl_2 . Samples were placed in mechanically scratched open clotting tips for 120 min, at room temperature, in a humidity chamber. A detailed description of the method can be seen in Supplementary Material.

Scanning electron microscopy

Scanning electron microscopy (SEM) was used to further investigate the structure of clots formed with $\gamma\text{A}\gamma\text{A}$ and $\gamma\text{A}\gamma'$ fibrinogen in the presence or in the absence of RBCs.

Clots were generated by adding 100 μl of $\gamma\text{A}\gamma\text{A}$ and $\gamma\text{A}\gamma'$ fibrinogen variants (final concentration of 1 mg/ml) to 10 μl of activation mixture (human thrombin 1 U/ml and 10 mM CaCl_2 , final concentrations, in TBS (50 mM Tris, 100 mM NaCl, pH 7.5)). All details of the procedure are described in Supplementary Material.

Laser scanning confocal microscopy

Fibrin clots were prepared according the procedure described in Supplementary Material. Three random areas of the clot were visualized under higher magnification. 20 μm optical z-stacks were obtained and projected into 2D images. In order to obtain 3D images of the fibrin clots, 40 μm z-stacks were also performed. Confocal microscopy was also used to assess, in real time, the rate of fibrinolysis following the procedure also described in Supplementary Material.

Statistical Analysis

Descriptive statistics are given as mean \pm standard error of mean (SEM). Unpaired Student's *t*-test was used for statistical analysis of comparisons between two groups. Non-parametric analysis was also performed in cell-cell adhesion data, applying the Mann Whitney U test. P-values below 0.05 were considered to indicate statistical significance. Statistical analyses were performed using GraphPad Prism 5 (La Jolla, CA, USA).

Results

RBC-RBC adhesion is altered in the presence of fibrinogen variants

Atomic force microscopy experiments were performed to investigate RBC cell-cell adhesion and the influence of $\gamma A\gamma'$ and $\gamma A\gamma A$ fibrinogen variants in the cells adhesion. We evaluated the interaction between RBCs, in the presence of different concentrations of $\gamma A\gamma A$ and $\gamma A\gamma'$ fibrinogen variants, up to 1.0 mg/ml, by force-distance retract curves (Figure 1).

AFM data showed that, in the presence of low concentrations of $\gamma A\gamma'$ fibrinogen, the work (thermodynamic parameter corresponding to the area under the curve on a force \times distance plot, Figure 1B) required to detach one RBC from another was higher than in the presence of the same concentration of $\gamma A\gamma A$ fibrinogen (0.87 ± 0.07 fJ vs. 0.55 ± 0.04 fJ, $p=0.0275$, for 0.1 mg/ml fibrinogen, and 1.03 ± 0.06 fJ vs. 0.65 ± 0.07 fJ, $p<0.0001$, for 0.4 mg/ml fibrinogen) (Figure 1C). At higher concentrations of fibrinogen variants, statistically significant differences between both variants were not observed (for 0.4 mg/ml fibrinogen, 0.71 ± 0.05 fJ for $\gamma A\gamma'$ vs. 1.10 ± 0.13 fJ for $\gamma A\gamma A$, $p=0.144$; for 0.7 mg/ml fibrinogen, 0.57 ± 0.07 fJ for $\gamma A\gamma'$ vs. 0.86 ± 0.04 fJ for $\gamma A\gamma A$, $p=0.248$). $\gamma A\gamma A$ fibrinogen concentrations showed a clear dose-response for interactions with RBCs, whereas $\gamma A\gamma'$ had a dual effect at low and high concentrations (Figure 1C). Values of the maximum detachment force (schematically explained in Figure 1B) were also calculated. As shown on Figure 1D, statistically significant differences between the values of maximum RBC-RBC detachment force in the presence of $\gamma A\gamma'$ or $\gamma A\gamma A$ fibrinogen were found at all fibrinogen concentrations: for 0.1 mg/ml fibrinogen, 141.8 ± 17.2 pN for $\gamma A\gamma A$ vs. 173.6 ± 0.85 pN for $\gamma A\gamma'$, $p = 0.0279$; for 0.4 mg/ml fibrinogen, 246.3 ± 5.64 pN for $\gamma A\gamma A$ vs. 203.7 ± 0.70 pN for $\gamma A\gamma'$, $p < 0.0001$; for 0.7 mg/ml fibrinogen, 141.2 ± 5.35 pN for $\gamma A\gamma A$ vs. 170.3 ± 0.95 pN for $\gamma A\gamma'$, $p < 0.0001$; and, for 1 mg/ml fibrinogen, 182.9 ± 9.80 pN for $\gamma A\gamma A$ vs. 205.5 ± 1.90 pN for $\gamma A\gamma'$, $p = 0.0054$). With the exception of the data obtained for 0.4 mg/ml fibrinogen, the values of maximum detachment force obtained for $\gamma A\gamma A$ fibrinogen were always lower than those of $\gamma A\gamma'$ fibrinogen.

After the initial maximum detachment force, two types of jumps could be observed on the force curves (Figure 1B): jumps preceded by a ramp of force or jumps preceded by a force plateau. We considered a membrane tether as a step in force detected after a force plateau of 0.25 μm in distance. Jump events were assigned to the unbinding of membrane ligand-receptor interactions without a preceding membrane deformation, while membrane tether events corresponded to situations where a membrane tether was extruded before the unbinding of the ligand-receptor complex (Figure 1B)³⁵. A combination of each of the parameters extracted from the force-distance curves (maximum detachment force, number of jumps events/curve \times mean force of jumps and number of membrane tethers events \times mean force of tethers) could be considered as the value of the work needed to detach one cell from another. Similarly to the values of work (Figure 1C), the same profile is observed for the values of force of jumps and membrane tethers events with increasing fibrinogen concentrations when comparing both fibrinogen variants As depicted in Figure 1E,F, at lower fibrinogen concentrations, jumps and membrane tethers displayed higher forces for $\gamma\text{A}\gamma'$ fibrinogen, when compared to $\gamma\text{A}\gamma\text{A}$ variant, both for 0.1 mg/ml fibrinogen (jumps, 68.52 ± 2.42 pN vs. 40.40 ± 0.80 pN, $p < 0.0001$; membrane tethers, 79.80 ± 7.06 pN vs. 47.56 ± 3.37 pN, $p < 0.0001$) and 0.4 mg/ml fibrinogen (jumps, 80.82 ± 3.45 pN vs. 74.94 ± 3.31 pN, $p = 0.0061$; membrane tethers, 91.91 ± 6.32 pN vs. 68.08 ± 9.69 pN, $p = 0.0069$). Figure 1E,F also shows that, at higher fibrinogen concentrations, similarly to the values of work, higher forces of jumps and membrane tethers were measured for $\gamma\text{A}\gamma\text{A}$ fibrinogen, when compared to the $\gamma\text{A}\gamma'$ variant. This becomes evident at 0.7 mg/ml of fibrinogen (jumps, 70.94 ± 4.36 pN vs. 24.01 ± 0.77 pN, $p < 0.0001$; membrane tethers, 117.75 ± 14.64 pN vs. 36.47 ± 5.13 pN, $p < 0.0001$) and at 1.0 mg/ml of fibrinogen (jumps, 201.51 ± 8.54 pN vs. 93.41 ± 2.85 pN, $p < 0.0001$; membrane tethers, 313.95 ± 58.05 pN vs. 135.51 ± 7.98 pN, $p > 0.05$).

RBCs influence $\gamma\text{A}\gamma'$ fibrin clot mechanical properties

The viscoelastic properties of $\gamma\text{A}\gamma\text{A}$ and $\gamma\text{A}\gamma'$ fibrin clots were examined using a magnetic microrheometer and the influence of RBCs was studied. In agreement with previous findings²²,

we observed that $\gamma A\gamma A$ clots were stiffer than $\gamma A\gamma'$ clots (storage modulus, G' , 1.076 ± 0.065 Pa vs. 0.512 ± 0.051 Pa, respectively; $p < 0.0001$; Figure 2). The presence of RBCs in the $\gamma A\gamma A$ fibrin clots did not statistically change their stiffness. On the other hand, a significant increase in the stiffness of $\gamma A\gamma'$ clots was observed in clots with RBCs, when compared to those without RBCs (1.220 ± 0.104 Pa vs. 0.512 ± 0.051 Pa, respectively; $p < 0.0001$). There were no significant differences on storage modulus G' between $\gamma A\gamma A$ and $\gamma A\gamma'$ clots in the presence of RBCs; however, there was a trend for the $\gamma A\gamma'$ clots to be stiffer than $\gamma A\gamma A$ clots (Figure 2).

In addition, we observed a statistically significant change on loss tangent ($\text{Tan } \delta$) comparing $\gamma A\gamma A$ clots with RBCs and without RBCs (0.460 ± 0.066 vs. 1.013 ± 0.126 , respectively; $p = 0.0008$), but only a trend for higher $\text{Tan } \delta$ in $\gamma A\gamma'$ with RBCs than for this variant in the absence of RBCs (data not shown).

RBCs reduce $\gamma A\gamma'$ fibrin clot permeability

To characterize the fibrin network of $\gamma A\gamma A$ and $\gamma A\gamma'$ fibrin with and without RBCs, permeability experiments were performed. The results for the Darcy constant (K_s), which represent the pore size of the fibrin clot, are shown in Figure 3.

Importantly, in the presence of RBCs, normalized K_s was higher for $\gamma A\gamma A$ fibrin clots with RBCs ($(2.44 \pm 0.3.1) \times 10^{-9}$ cm²) than for $\gamma A\gamma'$ fibrin clot with RBCs ($(1.40 \pm 0.10) \times 10^{-9}$ cm²) ($p = 0.0001$). Thus, when comparing clots of both fibrinogen variants with RBCs, the $\gamma A\gamma'$ clots were less porous.

RBCs influence $\gamma A\gamma A$ and $\gamma A\gamma'$ fibrin clot structure

Scanning electron microscopy data showed differences between the structures of the fibers formed by $\gamma A\gamma A$ or $\gamma A\gamma'$ fibrinogen (different magnification micrographs from each sample are shown in Figure S1 in the supplementary information).

We next investigated the structure of plasma clots formed *in vitro* in the presence of RBCs to determine the effect that these cells might have on clot structure *in vivo*. RBCs tended to be heterogeneously spread throughout the sample, particularly in clots produced with $\gamma A\gamma'$ fibrin

(Figure 4). Upon the addition of 20% RBCs, the structure of the $\gamma A\gamma'$ clot became more heterogeneous, with densely packed fiber regions as well as large holes where more RBCs were located (Figure 4 A, C, E). $\gamma A\gamma'$ fibrin fibers were thinner and the network of the clot showed more interconnections with RBCs compared to $\gamma A\gamma A$ fibers. On the micrographs of Figure 4 (panels B, D and F), it can be noticed that $\gamma A\gamma'$ fibrin clots contained more free fiber ends and there were more fiber-to-RBC points of connections, when compared to $\gamma A\gamma A$ fibrin clots, resulting in “clustered” cell arrangements.

In order to measure the diameter of the fibers, twenty fibers from 25000 \times magnification images were assessed on 2 different clots from each condition and in 3 different zones of the clot. Average fiber diameters were smaller in $\gamma A\gamma'$ fibrin compared to the $\gamma A\gamma A$ variant (18.29 ± 1.32 nm vs. 41.10 ± 1.58 nm, $p < 0.0001$; Figure 5). The presence of RBCs in the fibrin clot caused a decrease of the $\gamma A\gamma A$ fibers diameters compared to the clot without RBCs (41.10 ± 1.58 nm in the absence of RBCs vs. 35.39 ± 2.46 nm in their presence, $p = 0.044$) (Figure 5). The presence of RBCs on clots with $\gamma A\gamma'$ fibers did not statistically change the diameter of the fibers compared to the clots without cells. However, clots with RBCs and prepared with $\gamma A\gamma'$ fibrinogen led to thinner fibers than those produced with $\gamma A\gamma A$ fibrinogen and RBCs (35.39 ± 2.46 nm for $\gamma A\gamma A$ vs. 15.23 ± 0.98 nm for $\gamma A\gamma'$, $p < 0.0001$; Figure 5).

Increased fibrinolytic resistance of $\gamma A\gamma'$ fibrin clots in the presence of RBCs

We used laser scanning confocal microscopy to study clot structure and resistance to fibrinolysis in the presence and absence of RBCs for each fibrin variant.

Figure 6 shows representative examples of the confocal micrographs obtained for fiber clots made with $\gamma A\gamma A$ and $\gamma A\gamma'$ purified fibrinogen variants. In clots formed with $\gamma A\gamma A$ fibrinogen, the area occupied by the fibers seems to be larger (Figure 6A) than for the clots with $\gamma A\gamma'$ fibrinogen (Figure 6B). However, these differences were not statistically significant. In agreement with SEM imaging and with previous studies²², there was a clear difference between the structures of $\gamma A\gamma A$ and $\gamma A\gamma'$ fibrin. The $\gamma A\gamma A$ fibrin clots were composed of longer and straighter fibers than $\gamma A\gamma'$ fibrin clots. The later showed fibers that were shorter and clustered,

producing larger pores. However, we did not find differences regarding the fiber density comparing $\gamma A\gamma A$ with $\gamma A\gamma'$ fibrin clots (Figure S2).

Relevant was to study the micrographs of fibrin clots from $\gamma A\gamma A$ and $\gamma A\gamma'$ fibrinogen variants in the presence of 2% of RBCs, as shown on Figure 6 (C,D). In the presence of $\gamma A\gamma A$ fibrinogen, the network of the fibers seemed straighter and denser. In clots with $\gamma A\gamma'$ fibers, we observed that the fibers were more clustered and the RBCs were more visible. We also studied fibrin clots in the presence of 5% and 10% of RBCs by LSCM; however, the high number of RBCs did not allow clearly differentiating fibrin fibers from RBCs. Thus, technical limitations restricted us to increase the amount of RBCs closer to the physiological range.

Finally, we studied fibrinolysis of clots made with both fibrinogen variants (Figure 7). In line with previous studies²¹, a significant increase in lysis time was observed for $\gamma A\gamma'$ compared with $\gamma A\gamma A$ fibrin clots (15.82 ± 1.48 min vs. 10.54 ± 0.44 min, respectively; $p = 0.0267$). During the experiment, we observed a non-uniform lysis of the $\gamma A\gamma'$ fibrin clot, taking more time to achieve complete lysis than the $\gamma A\gamma A$ clot (videos in Supplementary information).

We measured the lysis time for $\gamma A\gamma A$ and $\gamma A\gamma'$ clots in the presence of 5% (data not shown) and 10% of RBCs. Under these conditions, there were no significant differences in fibrinolysis times in the presence of RBCs, when compared to the clots without RBCs. Statistical significance was observed in fibrinolysis times for $\gamma A\gamma A$ vs. $\gamma A\gamma'$ fibrin clots in the presence of RBCs (12.03 ± 0.49 min vs. 18.30 ± 1.47 min; $p = 0.0476$).

Discussion

In this study, we evaluated the interaction of purified $\gamma A\gamma'$ and $\gamma A\gamma A$ fibrinogen with RBCs, as well as their influence on the structure and function of clots formed with both variants. They show a discernible effect of the presence of RBCs on fibrin clot structure and function. To pursue this study further, we purified the main component of plasma fibrinogen, $\gamma A\gamma A$, and its splice-variant, $\gamma A\gamma'$. Cell-cell adhesion studies were performed to evaluate the relative roles of both fibrinogen variants on the interaction between RBCs. We also evaluated the changes of biophysical properties of the clots, by studying their permeability and viscoelastic properties. By laser confocal microscopy and scanning electron microscopy, we directly observed the effects of RBCs on the architecture of clots formed from $\gamma A\gamma'$ and $\gamma A\gamma A$ fibrinogens.

AFM data showed that in the presence of low concentrations of $\gamma A\gamma'$ fibrinogen (≤ 0.4 mg/ml), the force of the binding between two RBCs was higher than with $\gamma A\gamma A$ fibrinogen. Statistically significant differences between both fibrinogen variants at all fibrinogen concentrations were obtained for the values of force for the maximum cell-cell detachment, jumps and membrane tether events. Although these three parameters contribute to the values of the work necessary to completely detach two RBCs, no statistically significant variations were obtained for this parameter at fibrinogen concentrations ≥ 0.7 mg/mL.

Thus, at lower fibrinogen concentrations, $\gamma A\gamma'$ fibrinogen binds more promptly to RBCs, inducing higher RBC-RBC adhesion than $\gamma A\gamma A$ fibrinogen. RBCs adhesion has a clear $\gamma A\gamma A$ fibrinogen dose response curve, whereas $\gamma A\gamma'$ did not. This could be due to differences in fibrinogen variant molecular conformations and net protein electrostatic charge, which could lead to different binding affinities at different fibrinogen concentrations. It is known that RBCs present sialic acid residues on their surface, contributing to their negative surface charge, which induce repulsive electrostatic forces that minimize RBC aggregation under blood flow conditions³⁶. The binding of the more negatively charged γ' fibrinogen to RBCs may increase the overall negative cell surface charge. This may overcome the strong RBC-RBC interactions observed at lower $\gamma A\gamma'$ fibrinogen concentration, by lowering cell-cell adhesion forces, due to

increased electrostatic repulsion. On the other hand, $\gamma A\gamma A$ fibrinogen lacks the negatively charged sequence of γ' chain, leading to an increase of RBC-RBC adhesion upon increasing its concentration.

Previous studies have shown that RBCs influence the viscoelastic properties of the clot^{32, 37}. Our evaluation of the viscoelastic properties of the clots revealed that $\gamma A\gamma A$ fibrin clots are stiffer than $\gamma A\gamma'$ fibrin clots in the absence of RBCs, in agreement with previous studies on the effect of $\gamma A\gamma'$ on clot stiffness²². Our data shows that $\gamma A\gamma'$ clots are inherently weaker. This is likely due to differences in fibrin fiber structure. We recently demonstrated that fibrinogen γ' influences intrafibrillar structure of fibrin and significantly reduces the average number of protofibrils packed within the fibrin fiber, thereby influencing clot stiffness³⁸. In $\gamma A\gamma A$ fibrin clots, more protofibrils are packed within fibrin fibers, which increases the rigidity and the viscosity of the clot, when compared to $\gamma A\gamma'$ fibrin clots. In this study, the presence of RBCs did not influence the stiffness of the $\gamma A\gamma A$ fibrin clots. In $\gamma A\gamma'$ fibrin clots, the presence of RBCs resulted in a significant increase in stiffness. This indicates that the combination of $\gamma A\gamma'$ fibrinogen variant and RBCs may affect clot structure and mechanical properties. The stiffening of the $\gamma A\gamma'$ fibrin clots in the presence of RBCs may be related to rearrangements of protofibril packing or significant modifications in clot structure. The imaging by SEM of the clot structure in the presence of RBCs, compared to its absence, showed a looser structure in clots produced with $\gamma A\gamma'$ fibrinogen, which may be more prone to creep, as well as more fiber interconnections, which turn the clot more rigid. Our data indicates that RBCs are not a mere bystander in blood clot formation. Indeed, other studies have shown that RBCs influence fibrin network structure and pore size^{39, 40}. A decrease in the permeability of fibrin clots after the addition of RBCs was shown to be proportional to the total RBC surface area and their total concentration⁴⁰. Here, we show that the addition of RBCs promotes the decrease of permeability. Importantly, we show that the $\gamma A\gamma'$ clots with RBCs were less porous than $\gamma A\gamma A$ clots with RBCs. This could potentially lead to pro-thrombotic clots, due to a higher resistance to fibrinolysis⁴¹. In agreement with this, we also found an increase in the lysis time of $\gamma A\gamma'$ clots with RBCs, when compared to $\gamma A\gamma A$ clots with RBCs.

According with previous studies^{22, 23}, SEM and confocal microcopy showed that the clots formed by $\gamma A\gamma A$ and $\gamma A\gamma'$ fibers have a different structure. The incorporation of RBCs has an important impact on fibrin fiber size and in its network structure. Regions of higher and lower RBC density were clearly visible in the clots made with γ' fibrinogen. In the presence of RBCs, the γ' fibrin clots were more heterogeneous, seeming to form a looser structure when compared with the clots of γA fibrinogen. These findings are supported by our AFM data. At high $\gamma A\gamma'$ fibrinogen concentrations, the work necessary to detach two RBCs was the same that the one achieved in the presence of $\gamma A\gamma A$ fibrinogen. In agreement with this, the clot might become looser, with a higher ability to deform and embolise, eventually blocking a downstream blood capillary.

The $\gamma A\gamma'$ fibrin clots contain a large number of free fiber ends. Fiber ends are normally found at low levels in scanning electron micrographs of fibrin clots, and have been suggested to arise from early truncation of protofibril formation or lateral aggregation^{42, 43}. It was previously proposed that the negative charge of $\gamma A\gamma'$ fibrinogen on the D-D interface may disrupt oligomerization and, therefore, interrupt the continuous growth of the protofibril, leading to highly branched fibers^{44, 45}.

This study has shown that the incorporation of RBCs into the clot affects fibrin fiber formation. RBCs induced thinning of fibers in fibrin clots formed with $\gamma A\gamma A$, but not with $\gamma A\gamma'$ fibrinogen. However, in the presence of RBCs, $\gamma A\gamma A$ fibers remained significantly thicker than $\gamma A\gamma'$ fibers. Here, we could conclude that thinner fibrin fibers (such as $\gamma A\gamma'$ fibrin fibers) form highly branched networks. We propose that growing fibers surround RBCs, interacting with them through an RBC surface receptor. We have already reported the existence of a receptor for fibrinogen on RBCs^{29, 30, 31}: RBCs specifically bind fibrin(ogen) via an integrin receptor with a β_3 subunit²⁹, possibly $\alpha_v\beta_3$ ³¹.

Previous studies indicated that fibrin clots with increased fiber branching and resistance to fibrinolysis are a risk factor for thrombosis¹⁵. Fibrinolysis data showed that the lysis time of a $\gamma A\gamma'$ fibrin clot is longer than for a $\gamma A\gamma A$ clot, as already reported^{4, 5}. The presence of RBCs seems to increase the lysis time. However these studies were conducted with a 10% hematocrit,

due to technical limitations, considerably below the normal hematocrit of ~40% RBCs. Aleman *et al.* and Tutwiler *et al.* suggested that RBCs cause direct and complex effects on clot structure and stability^{46,47}. Furthermore, RBCs can support thrombin generation and decrease fibrinolysis, suggesting that RBCs may promote fibrin deposition during venous thrombosis⁴⁶. Other authors report the role of RBCs on stabilizing clots based on suppressed tissue plasminogen activator(tPA)-induced fibrinolysis in RBC-modified fibrin structures. They also observed, using eptifibatide inhibition, that RBCs modulate fibrinolysis through a specific fibrinogen receptor⁴¹. Collet *et al.* demonstrated that fibrin clots with a tight fibrin conformation made of thinner fibers were lysed at a slower rate than those with a loose fibrin conformation made of thicker fibers, although the overall fibrin content remained constant⁴⁸. The $\gamma A\gamma'$ clot is more heterogeneous than the $\gamma A\gamma A$ clot. The densely packed areas with fibers and RBCs may impair the diffusion of fibrinolytic agents. However, at the same time, there are areas with large holes, where their diffusion may be increased. It was suggested that the slower lysis of γ' clots is due to delayed fibrinopeptide B release, leading to a delay of plasminogen binding and activation²¹. Some of these findings may provide a mechanism underpinning the epidemiological data suggesting that a high ratio between $\gamma A\gamma'$ and $\gamma A\gamma A$ fibrinogen variants may be a risk factor for thrombotic disease^{7,8,9}. Further studies on the prothrombotic nature of RBCs and on fibrinogen variants are necessary to fully understand the contribution of the γ' chain and RBCs to different etiologies of thrombotic diseases.

In conclusion, the incorporation of RBCs into a fibrin clot significantly affects the clot structure and its mechanical properties. RBCs interact differently with clots made with γ -chain fibrinogen splice variants, which may explain some of the cardiovascular clinical associations that have been reported with these fibrinogen variants.

References

1. Brown JH, Volkmann N, Jun G, Henschen-Edman AH, Cohen C. The crystal structure of modified bovine fibrinogen. *Proc Natl Acad Sci U S A* 2000; **97**: 85-90.
2. Chung DW, Davie EW. gamma and gamma' chains of human fibrinogen are produced by alternative mRNA processing. *Biochemistry* 1984; **23**: 4232-6.
3. Mosesson MW, Finlayson JS, Umfleet RA. Human fibrinogen heterogeneities. 3. Identification of chain variants. *J Biol Chem* 1972; **247**: 5223-7.
4. Collet JP, Nagaswami C, Farrell DH, Montalescot G, Weisel JW. Influence of gamma' fibrinogen splice variant on fibrin physical properties and fibrinolysis rate. *Arterioscler Thromb Vasc Biol* 2004; **24**: 382-6.
5. Falls LA, Farrell DH. Resistance of gammaA/gamma' fibrin clots to fibrinolysis. *J Biol Chem* 1997; **272**: 14251-6.
6. Siebenlist KR, *et al.* Studies on the basis for the properties of fibrin produced from fibrinogen-containing gamma' chains. *Blood* 2005; **106**: 2730-6.
7. Lovely RS, *et al.* Association of gammaA/gamma' fibrinogen levels and coronary artery disease. *Thromb Haemost* 2002; **88**: 26-31.
8. Mannila MN, *et al.* Elevated plasma fibrinogen gamma' concentration is associated with myocardial infarction: effects of variation in fibrinogen genes and environmental factors. *J Thromb Haemost* 2007; **5**: 766-73.
9. Cheung EY, *et al.* Fibrinogen gamma' in ischemic stroke: a case-control study. *Stroke* 2008; **39**: 1033-5.
10. Mosesson MW, *et al.* Plasma fibrinogen gamma' chain content in the thrombotic microangiopathy syndrome. *J Thromb Haemost* 2007; **5**: 62-9.
11. Uitte de Willige S, de Visser MC, Houwing-Duistermaat JJ, Rosendaal FR, Vos HL, Bertina RM. Genetic variation in the fibrinogen gamma gene increases the risk for deep venous thrombosis by reducing plasma fibrinogen gamma' levels. *Blood* 2005; **106**: 4176-83.
12. Appiah D, Schreiner PJ, MacLehose RF, Folsom AR. Association of Plasma gamma' Fibrinogen With Incident Cardiovascular Disease: The Atherosclerosis Risk in Communities (ARIC) Study. *Arterioscler Thromb Vasc Biol* 2015; **35**: 2700-6.

13. Walton BL, Getz TM, Bergmeier W, Lin FC, Uitte de Willige S, Wolberg AS. The fibrinogen gammaA/gamma' isoform does not promote acute arterial thrombosis in mice. *J Thromb Haemost* 2014; **12**: 680-9.
14. Fuster V, Moreno PR, Fayad ZA, Corti R, Badimon JJ. Atherothrombosis and high-risk plaque: part I: evolving concepts. *J Am Coll Cardiol* 2005; **46**: 937-54.
15. Undas A, Ariens RA. Fibrin clot structure and function: a role in the pathophysiology of arterial and venous thromboembolic diseases. *Arterioscler Thromb Vasc Biol* 2011; **31**: e88-99.
16. Weisel JW. Structure of fibrin: impact on clot stability. *J Thromb Haemost* 2007; **5** Suppl 1: 116-24.
17. Weisel JW. The mechanical properties of fibrin for basic scientists and clinicians. *Biophys Chem* 2004; **112**: 267-76.
18. Collet JP, et al. Dusart syndrome: a new concept of the relationship between fibrin clot architecture and fibrin clot degradability: hypofibrinolysis related to an abnormal clot structure. *Blood* 1993; **82**: 2462-9.
19. Bridge KI, Philippou H, Ariens R. Clot properties and cardiovascular disease. *Thromb Haemost* 2014; **112**: 901-8.
20. Carter AM, Cymbalista CM, Spector TD, Grant PJ. Heritability of clot formation, morphology, and lysis: the EuroCLOT study. *Arterioscler Thromb Vasc Biol* 2007; **27**: 2783-9.
21. Kim PY, Vu TT, Leslie BA, Stafford AR, Fredenburgh JC, Weitz JI. Reduced plasminogen binding and delayed activation render gamma'-fibrin more resistant to lysis than gammaA-fibrin. *J Biol Chem* 2014; **289**: 27494-503.
22. Allan P, Uitte de Willige S, Abou-Saleh RH, Connell SD, Ariens RA. Evidence that fibrinogen gamma' directly interferes with protofibril growth: implications for fibrin structure and clot stiffness. *J Thromb Haemost* 2012; **10**: 1072-80.
23. Cooper AV, Standeven KF, Ariens RA. Fibrinogen gamma-chain splice variant gamma' alters fibrin formation and structure. *Blood* 2003; **102**: 535-40.
24. Lovely RS, Moaddel M, Farrell DH. Fibrinogen gamma' chain binds thrombin exosite II. *J Thromb Haemost* 2003; **1**: 124-31.

25. Fredenburgh JC, Stafford AR, Leslie BA, Weitz JI. Bivalent binding to gammaA/gamma'-fibrin engages both exosites of thrombin and protects it from inhibition by the antithrombin-heparin complex. *J Biol Chem* 2008; **283**: 2470-7.
26. de Moerloose P, Boehlen F, Neerman-Arbez M. Fibrinogen and the risk of thrombosis. *Semin Thromb Hemost* 2010; **36**: 7-17.
27. Schmid-Schonbein H, Wells R, Goldstone J. Influence of deformability of human red cells upon blood viscosity. *Circ Res* 1969; **25**: 131-43.
28. Lominadze D, Dean WL, Tyagi SC, Roberts AM. Mechanisms of fibrinogen-induced microvascular dysfunction during cardiovascular disease. *Acta Physiol (Oxf)* 2010; **198**: 1-13.
29. Carvalho FA, *et al.* Atomic force microscopy-based molecular recognition of a fibrinogen receptor on human erythrocytes. *ACS Nano* 2010; **4**: 4609-20.
30. Carvalho FA, de Oliveira S, Freitas T, Goncalves S, Santos NC. Variations on fibrinogen-erythrocyte interactions during cell aging. *PLoS One* 2011; **6**: e18167.
31. Guedes AF, Carvalho FA, Malho I, Lousada N, Sargento L, Santos NC. Atomic force microscopy as a tool to evaluate the risk of cardiovascular diseases in patients. *Nat Nanotechnol* 2016; **11**: 687-92.
32. Gersh KC, Nagaswami C, Weisel JW. Fibrin network structure and clot mechanical properties are altered by incorporation of erythrocytes. *Thromb Haemost* 2009; **102**: 1169-75.
33. Evans RM, Tassieri M, Auhl D, Waigh TA. Direct conversion of rheological compliance measurements into storage and loss moduli. *Phys Rev E Stat Nonlin Soft Matter Phys* 2009; **80**: 012501.
34. Pieters M, Undas A, Marchi R, De Maat MP, Weisel J, Ariens RA. An international study on the standardization of fibrin clot permeability measurement: methodological considerations and implications for healthy control values. *J Thromb Haemost* 2012; **10**: 2179-81.
35. Ribeiro AS, *et al.* Atomic force microscopy and graph analysis to study the P-cadherin/SFK mechanotransduction signalling in breast cancer cells. *Nanoscale* 2016; **8**: 19390-401.

36. Fernandes HP, Cesar CL, Barjas-Castro Mde L. Electrical properties of the red blood cell membrane and immunohematological investigation. *Rev Bras Hematol Hemoter* 2011; **33**: 297-301.
37. Carr ME, Jr., Hardin CL. Fibrin has larger pores when formed in the presence of erythrocytes. *Am J Physiol* 1987; **253**: H1069-73.
38. Domingues MM, *et al.* Thrombin and fibrinogen gamma' impact clot structure by marked effects on intrafibrillar structure and protofibril packing. *Blood* 2016; **127**: 487-95.
39. Cines DB, *et al.* Clot contraction: compression of erythrocytes into tightly packed polyhedra and redistribution of platelets and fibrin. *Blood* 2014; **123**: 1596-603.
40. van Gelder JM, Nair CH, Dhall DP. The significance of red cell surface area to the permeability of fibrin network. *Biorheology* 1994; **31**: 259-75.
41. Wohner N, *et al.* Lytic resistance of fibrin containing red blood cells. *Arterioscler Thromb Vasc Biol* 2011; **31**: 2306-13.
42. Woodhead JL, Nagaswami C, Matsuda M, Arocha-Pinango CL, Weisel JW. The ultrastructure of fibrinogen Caracas II molecules, fibers, and clots. *J Biol Chem* 1996; **271**: 4946-53.
43. Hamano A, *et al.* Thrombophilic dysfibrinogen Tokyo V with the amino acid substitution of gammaAla327Thr: formation of fragile but fibrinolysis-resistant fibrin clots and its relevance to arterial thromboembolism. *Blood* 2004; **103**: 3045-50.
44. Macrae FL, Domingues MM, Casini A, Ariens RA. The (Patho)physiology of Fibrinogen gamma'. *Semin Thromb Hemost* 2016.
45. Gersh KC, Nagaswami C, Weisel JW, Lord ST. The presence of gamma' chain impairs fibrin polymerization. *Thromb Res* 2009; **124**: 356-63.
46. Aleman MM, Walton BL, Byrnes JR, Wolberg AS. Fibrinogen and red blood cells in venous thrombosis. *Thromb Res* 2014; **133 Suppl 1**: S38-40.
47. Tutwiler V, *et al.* Kinetics and mechanics of clot contraction are governed by the molecular and cellular composition of the blood. *Blood* 2016; **127**: 149-59.
48. Collet JP, *et al.* Influence of fibrin network conformation and fibrin fiber diameter on fibrinolysis speed: dynamic and structural approaches by confocal microscopy. *Arterioscler Thromb Vasc Biol* 2000; **20**: 1354-61.

Figure legends

Figure 1 | AFM cell-cell adhesion data. A) Schematic representation of the adhesion between two RBCs (one chemically attached to the cantilever and the other on the poly-L-lysine-treated substrate) in the presence of fibrinogen variants. B) Representative force-distance curve with the relevant analyzed parameters, namely, work of cell-cell detachment (grey area), maximum detachment force, jumps and membrane tethers (insets magnify examples of a jump and a membrane tether event on the force-distance curve). C) Work necessary to overcome RBC-RBC adhesion in the presence of different concentrations of $\gamma A\gamma A$ or $\gamma A\gamma'$ fibrinogen (*, $p = 0.0275$; ***, $p < 0.0001$). D) Maximum detachment force values to detach two RBCs (*, $p = 0.0279$; **, $p = 0.0054$; ***, $p < 0.0001$). E) Jumps and F) membrane tethers force data (**, $p \leq 0.0069$; ***, $p < 0.0001$) in the presence of each fibrinogen variant or in their absence. Values are presented as mean \pm standard error of mean (SEM).

Figure 2 | Viscoelastic properties of the purified $\gamma A\gamma A$ and $\gamma A\gamma'$ fibrinogen clots. Storage modulus G' (elastic modulus) data are presented in the presence of 0.5 % RBCs and in the absence of RBCs (***, $p < 0.0001$ for $\gamma A\gamma A$ vs. $\gamma A\gamma'$ and for $\gamma A\gamma'$ vs. $\gamma A\gamma' + RBC$). Fibrinogen concentration was 0.5 mg/ml. Values are presented as mean \pm SEM.

Figure 3 | Normalized permeability data (normalized in percentage against K_s of each variant without RBCs) in the presence of RBCs for fibrin clots formed with purified $\gamma A\gamma A$ or $\gamma A\gamma'$ fibrinogen. Darcy constant, K_s , represents the average size of the pores within the clot (*, $p = 0.0319$). Values are presented as mean \pm SEM.

Figure 4 | Scanning electron micrographs of fibrin fiber clots with 20% of RBCs. Fibers were formed from 1.0 mg/ml fibrinogen variants $\gamma A\gamma A$ (A, C and E) and $\gamma A\gamma'$ (B, D and F). White arrows in A indicate the more homogeneous structure in the $\gamma A\gamma A$ clot network, when compared with the areas of small and large holes, pinpointed by red arrows in B, associating a more heterogeneous structure to the $\gamma A\gamma'$ clots. The free fiber ends and the fiber-to-RBC points of connections are represented as small circles, being more frequent for $\gamma A\gamma'$ (red circles in F) than for $\gamma A\gamma A$ (white circles in E). Magnifications: A and B, 2500 \times ; C and D, 5000 \times ; E and F, 25000 \times .

Figure 5 | Diameters of purified $\gamma A\gamma A$ and $\gamma A\gamma'$ fibrin fibers in the absence or in the presence of 20% of RBCs. Fiber diameters were measured from 20 random fibers of each image using a 25000 \times magnification (*, $p = 0.0439$; ***, $p < 0.0001$).

Figure 6 | Laser scanning confocal microscopy images of fiber clots formed with purified $\gamma A\gamma A$ (A and C) and $\gamma A\gamma'$ (B and D) fibrinogen, at 1.0 mg/ml fibrinogen concentration. Alexa 488-labelled fibrin fibers are shown in green. Confocal micrographs of fiber clots with 2% of RBCs formed with 1.0 mg/ml of purified $\gamma A\gamma A$ (C) and $\gamma A\gamma'$ fibrinogen (D). Alexa 488-labelled fibrin fibers are shown in green. RBCs were labeled with Vibrant DiD cell-labeling solution (red). Z-stack images at 40 μm and 63 \times magnification are shown in panel A and B and Z-stacks images at 20 μm , also with 63 \times magnification are shown in panels C and D.

Figure 7 | Fibrinolysis time rates were assessed by laser scanning confocal microscopy from clots formed with purified $\gamma A\gamma A$ and $\gamma A\gamma'$ fibrinogen, in the absence and presence of RBCs (10%). The serial time scans were taken with 40 \times magnification. Values are shown as mean \pm SEM (*, $p \leq 0.0476$).

Figures

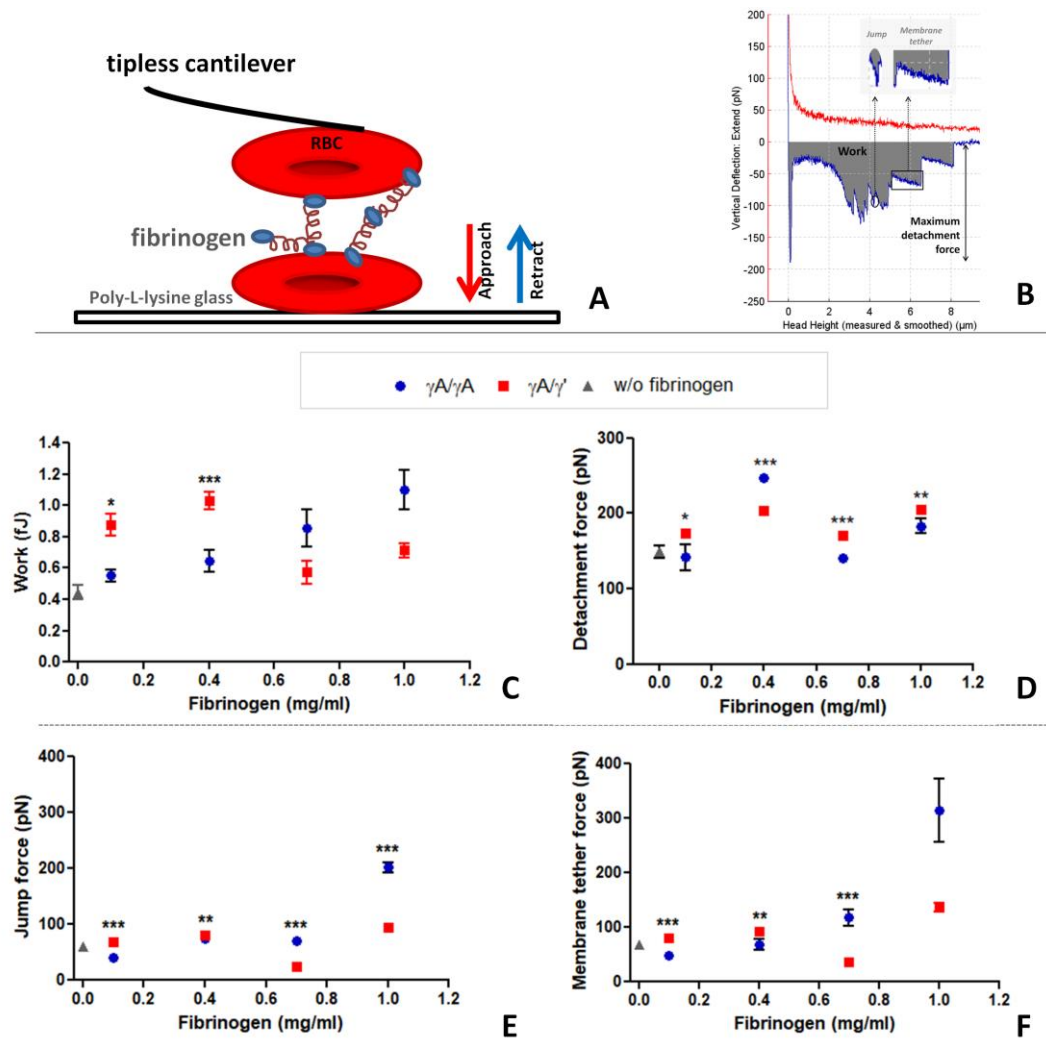


Figure 1

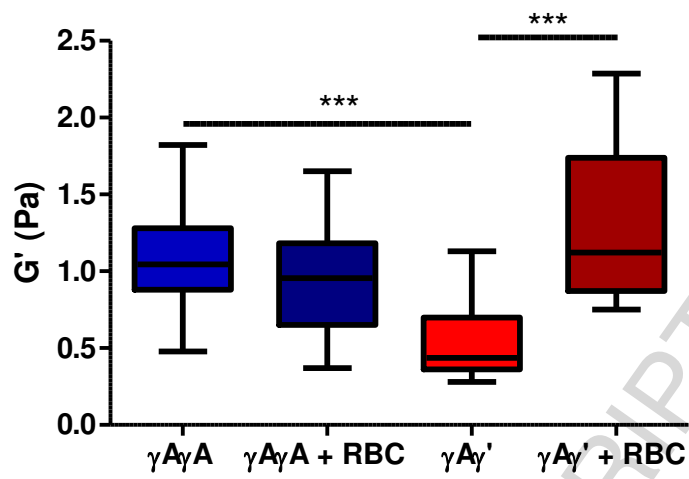


Figure 2

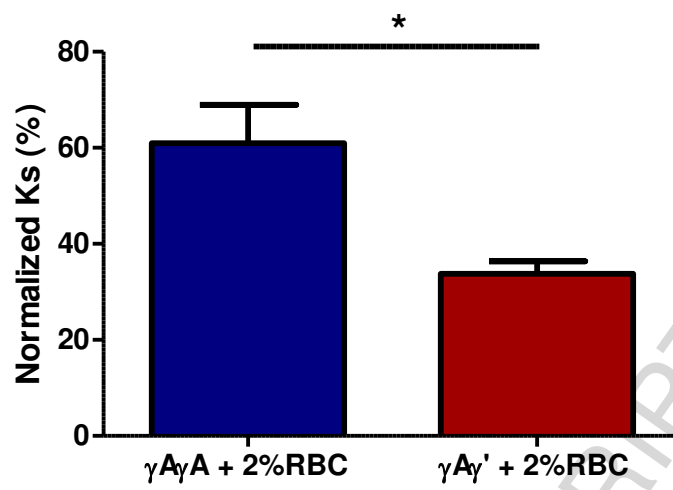


Figure 3

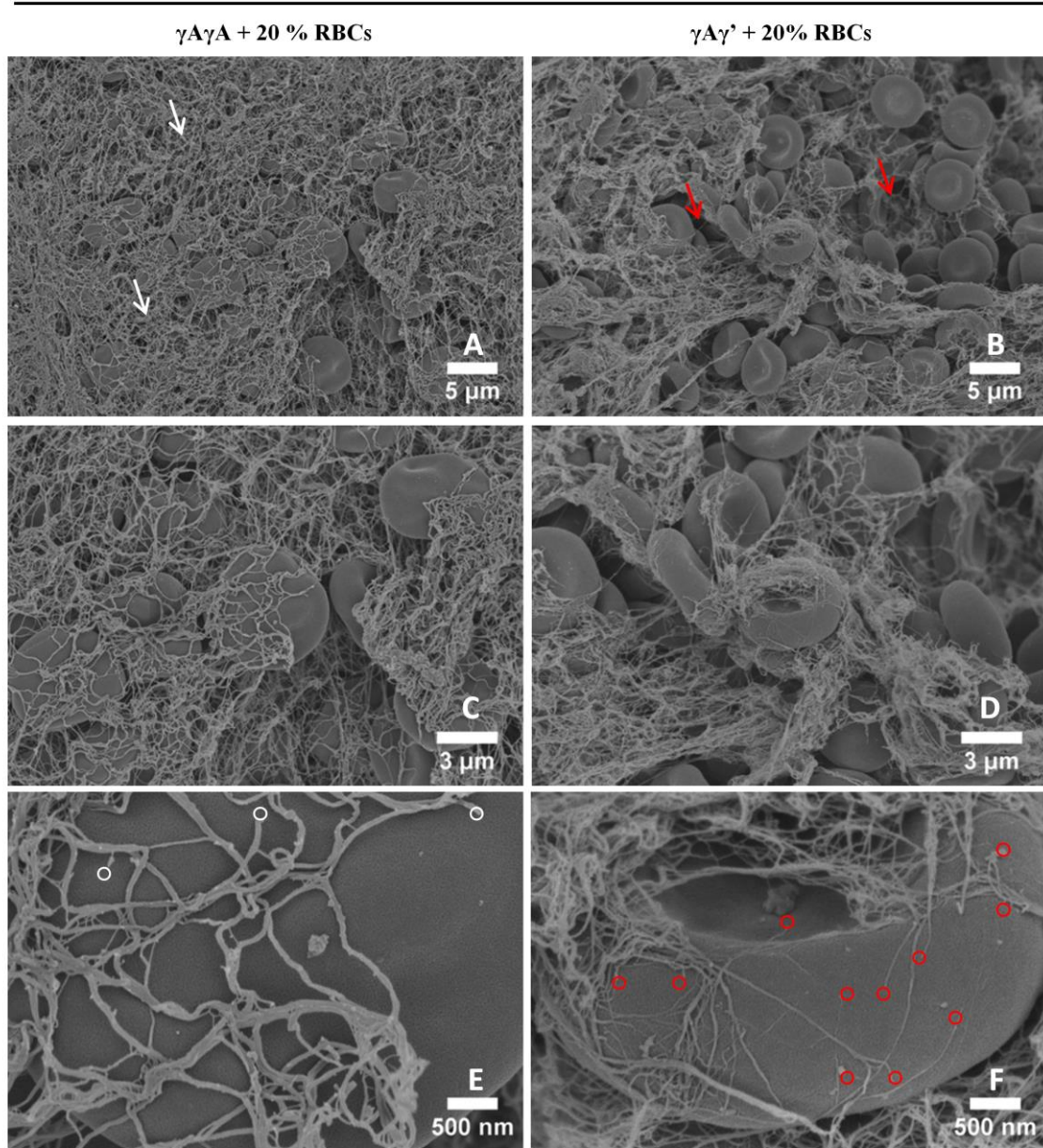


Figure 4

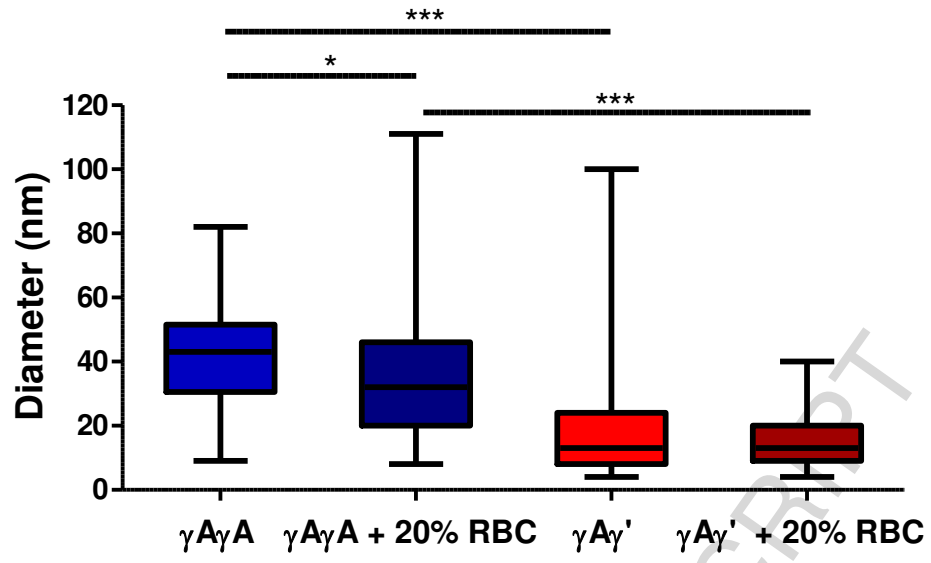


Figure 5

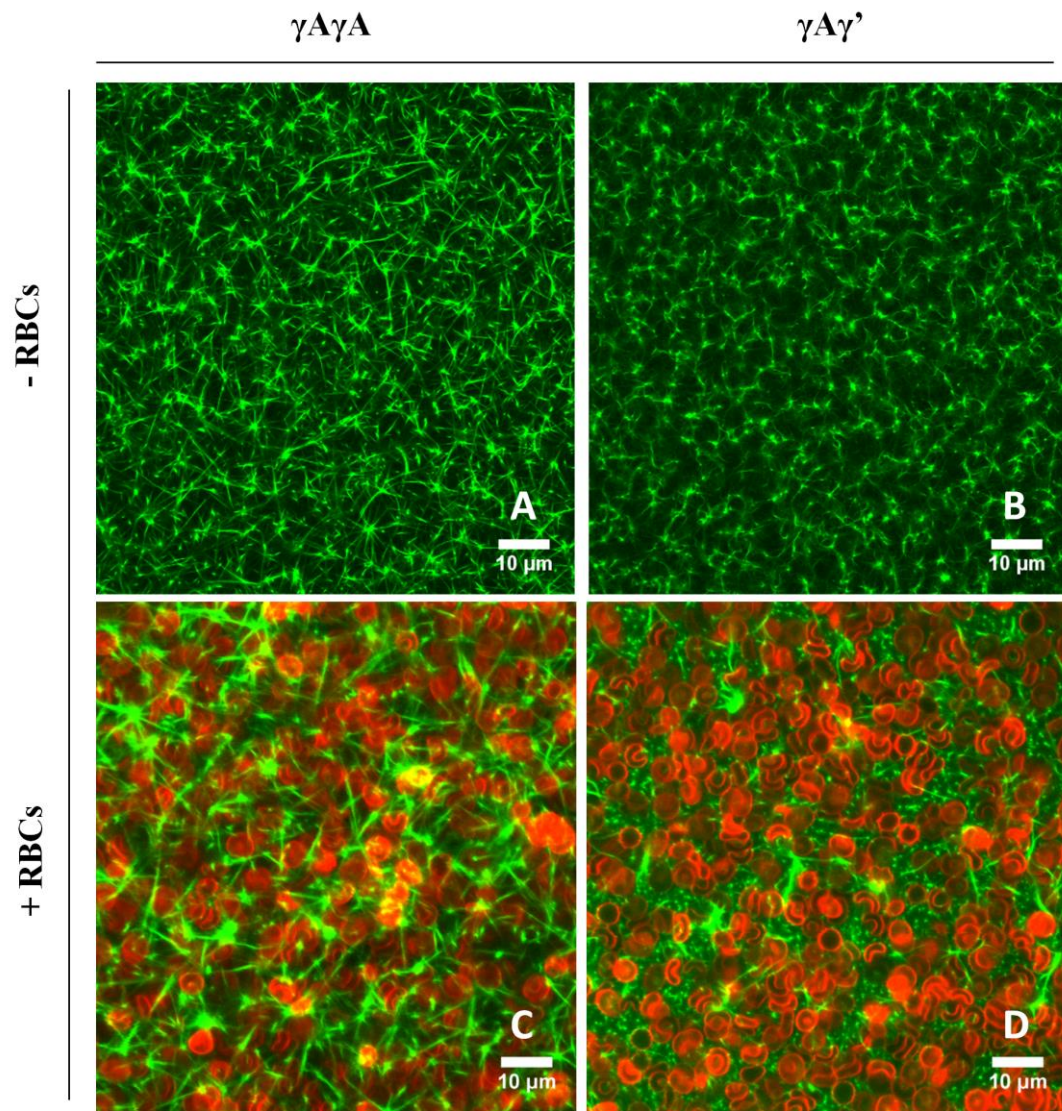


Figure 6

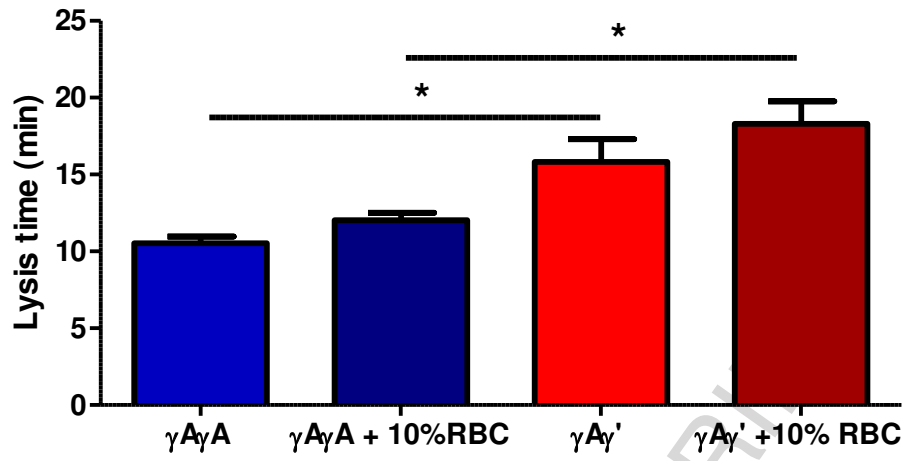


Figure 7

Graphical abstract description

Comparison of the interaction between red blood cells (RBCs) and $\gamma A\gamma A$ or $\gamma A\gamma'$ fibrinogen. Schematic representation of the adhesion forces between two RBCs in the presence of $\gamma A\gamma'$ fibrinogen, which affects clot properties and function. Changes on fibrin network structure, decreased fiber diameter, increased fibrinolysis and decreased permeability by $\gamma A\gamma'$ fibrinogen-RBC interactions were encountered. The nanotechnology-based approach was essential to understand that the RBCs interact differently with clots made with γ' chain fibrinogen splice variant instead of the common variant, γA . This may explain some of the cardiovascular clinical associations that have been reported for γ' fibrinogen.

